Konrad BOJAR[1], Vladimir ALSHITS[2,3], Jerzy P. NOWACKI[2], Aldona DRABIK[2], Romuald KOTOWSKI[2,4]

Industrial Research Institute for Automation and Measurements (1), Polish-Japanese Institute of Information Technology (2), Institute of Crystallography RAS (3), The State College of Computer Science and Business Administration (4)

Electro-elastostatic fields of dislocation in piezoelectric plate

Abstract. *We present in a form of 2D color-coded plots the results of computer simulations of electromechanical properties of a thin piezoelectric plate with a generalized linear defect. A typical example of a device with such plate is an immersion transducer in which one side of the active piezoelectric layer is clamped to a substrate and the other is mechanically free. Therefore we restrict ourselves to mixed boundary conditions.*

Streszczenie. *Prezentujemy wyniki w postaci kolorowych wykresów z komputerowych symulacji właściwości elektromechanicznych cienkiej płyty piezoelektrycznej z uogólnionym defektem liniowym. Przykładem urządzenia z taką płytą jest przetwornik zanurzeniowy, w którym jedna strona warstwy aktywnej jest zamocowana do substratu, a druga strona jest swobodna. Dlatego ograniczamy się do mieszanych warunków brzegowych.* (***Pola elektroelastyczne od dyslokacji w płytach piezoelektrycznych***)

Keywords: piezoelectricity, generalized linear defects, Stroh formalism, computer simulations.
Słowa kluczowe: piezoelektryczność, uogólnione defekty liniowe, formalizm Stroh, symulacje komputerowe.

Introduction

Due to rapid development of fabrication technologies, recently rising interest in thin-film piezoelectric structures of dimensions on the order of $1\ \mu m$ or even less is observed. At this scale practically all defects of crystal lattice become important: line forces, line charges, electric potential jumps, and dislocations [1, 2]. A lot of effort has been put into calculating the physical fields induced by such defects, also numerically [3]. Although static defects in a single layer with various boundary conditions have already been investigated (see bibliography of [2]), to the best of authors' knowledge, the solutions for mixed boundary conditions has never been visualized in 2D yet. In this paper we are going to fill this gap and give 2D plots of electro-elastostatic fields induced by a dislocation and a line force in GaAs. This should allow engineers to get an outline of magnitudes of parasitic fields and take them into account during development of new NDT heads, transducers, or other electronic elements, such as GaAs/GaAlAs heterojunctions in which GaAs usually forms outer layers.

Electro-elastic fields in the piezoelectric plate

The piezoelectric plate of thickness d with a cross-section chosen as the XY plane is considered (Fig. 1). The coordinates of the generalized linear defect parallel to the Z axis are (x', y'). The anisotropic material of the plate is characterized by the elastic moduli tensor c_{ijkl}, the piezoelectric constants e_{ikl}, and the electric permittivity ε_{ij}. The constitutive relations are assumed in the following form:

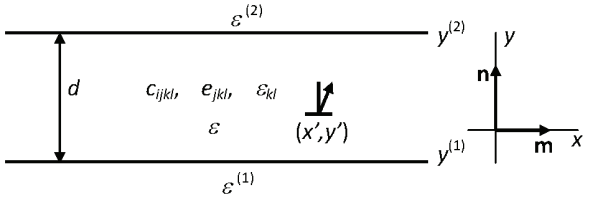

Fig.1. Geometry of the problem and choice of the coordinate system.

(1) $\sigma_{ij} = c_{ilkl}\,\beta_{kl} - e_{lij}\,E_l$,

(2) $D_j = e_{jkl}\,\beta_{kl} + \varepsilon_{jl}\,E_l$,

where σ_{ij} is the stress tensor, and D_j is the electric displacement vector. In presence of a line defect of the crystal lattice (the dislocation and the electrostatic line defect) the elastic distortion β_{kl} and the electric field E_l are not equal to gradients of the displacement vector $\boldsymbol{u}$ and the electric potential φ, respectively. In that case one has

(3) $u_{l,k} = \beta_{kl} + \beta^0_{kl}$,

(4) $-\varphi_{,k} = E_k - E^0_k$,

where

(5) $\boldsymbol{\beta}^0 = -\boldsymbol{b} \otimes \boldsymbol{n}\, H(x-x')\,\delta(y-y'),\ \boldsymbol{E}^0 = -\Delta\varphi\, \boldsymbol{n}\, H(x-x')\,\delta(y-y')$,

and $\boldsymbol{b}$ is the Burgers vector of the dislocation, $\boldsymbol{n}$ is the unit vector along the y-axis, $\Delta\varphi$ is the electric potential jump on the line defect, $H(x-x')$ is the Heaviside function, $\delta(y-y')$ is the Dirac distribution, and $\otimes$ denotes the tensor product. In this case the equilibrium equations are of the following form

(6) $\sigma_{ij,j} = -f_i\,\delta(x-x')\,\delta(y-y')$,

(7) $D_{j,j} = q\,\delta(x-x')\,\delta(y-y')$,

where $\boldsymbol{f}$ is the line force introduced by the defect, and q is the line charge. In our calculations an extension of the Stroh formalism [4] to the case of piezoelectricity introduced by Barnett and Lothe [5] is used. This formalism reduces the problem to a purely algebraic procedure of finding eigenvalues p_α and eigenvectors $\boldsymbol{\xi}_\alpha$ of some 8×8 matrix followed by some lengthy but simple algebraic operations. Below all the necessary notation and the final result of this formalism is introduced.

Stroh-Barnett-Lothe formalism

The starting point is the eight-dimensional equation [1]

(8) $(\boldsymbol{I}\partial_y - \boldsymbol{N}\partial_x)\boldsymbol{\eta}(x, y) = -\boldsymbol{g}\, H(x - x')\,\delta(y - y')$,

where $\boldsymbol{g}$ is the generalized line defect strength, $\boldsymbol{I}$ is the eight-dimensional identity matrix, $\boldsymbol{N}$ is the 8×8 matrix depending on the orientation of the frame $\{\boldsymbol{m}, \boldsymbol{n}\}$ and on the material constants of the strip

(9) $$\boldsymbol{N} = -\begin{pmatrix} (\boldsymbol{nn})^{-1}(\boldsymbol{nm}) & (\boldsymbol{nn})^{-1} \\ (\boldsymbol{mn})(\boldsymbol{nn})^{-1}(\boldsymbol{nm}) - (\boldsymbol{mm}) & (\boldsymbol{mn})(\boldsymbol{nn})^{-1} \end{pmatrix},$$

where $(\boldsymbol{mn})$ is the convolution operator defined by

(10) $(\boldsymbol{mn})_{KM} = \boldsymbol{m}_i\, C_{iKMj}\, \boldsymbol{n}_j$,

and C_{iJKl} are the generalized elastic moduli

(11) $$\begin{aligned} C_{iJKl} &= c_{ijkl} \quad \text{for} \quad J, K = j, k = 1,2,3, \\ &= e_{lij} \quad \text{for} \quad J = j = 1,2,3,\ K = 4, \\ &= e_{ikl} \quad \text{for} \quad J = 4,\ K = k = 1,2,3, \\ &= -\varepsilon_{il} \quad \text{for} \quad J = 4,\ K = 4, \end{aligned}$$

with an obvious symmetry

(12) $C_{iJKl} = C_{lKJi}$.

With this notations our Eqs. (1) and (2) can be rewritten in a shorter form

(13) $\Sigma_{iJ} = C_{iJKl}\, U_{lK}$.

with four-dimensional generalized displacements

(14) $$U_K = \begin{cases} u_k & K = k = 1,2,3 \\ \varphi & K = 4 \end{cases},$$

generalized stresses Σ_{iJ} and generalized elastic U_{lK} and plastic U^0_{lK} distortions given by [2]

(15) $$\Sigma_{iJ} = \begin{cases} \sigma_{ij} & J = j = 1,2,3 \\ D'_i & J = 4 \end{cases},$$

(16) $$U_{lK} = \begin{cases} \beta_{lk} & K = k = 1,2,3 \\ -E'_l & K = 4 \end{cases},$$

(17) $$U^0_{lK} = \begin{cases} \beta^0_{lk} & K = k = 1,2,3 \\ -E^0_l & K = 4 \end{cases},$$

In the Fourier representation the Eq. (8) takes the form

(18) $(\boldsymbol{I}\partial_y - \boldsymbol{N}\partial_x)\boldsymbol{\eta}(x, y) = -\boldsymbol{g}\,(2\pi i k)^{-1}\delta(y)$,

The eigenvectors $\boldsymbol{\xi}_\alpha$ and the eigenvalues p_α of the matrix $\boldsymbol{N}$

(19) $\boldsymbol{N}\,\boldsymbol{\xi}_\alpha = p_\alpha\,\boldsymbol{\xi}_\alpha$

form four pairs of complex conjugates. Therefore, without any loss of generality we can impose the following numbering

(20) $\boldsymbol{\xi}_{\alpha+4} = \boldsymbol{\xi}_\alpha^*$, $p_{\alpha+4} = p_\alpha^*$, $\alpha = 1,2,3,4,$

(21) $Im\, p_\alpha > 0$ for $\alpha = 1,2,3,4;$ $Im\, p_\alpha < 0$ for $\alpha = 5,6,7,8.$

The Stroh eigenvectors $\boldsymbol{\xi}_\alpha$ are orthogonal and complete which means that the subsequent relations hold

(22) $$\boldsymbol{\xi}_\alpha \cdot \boldsymbol{T}\,\boldsymbol{\xi}_\beta = \delta_{\alpha\beta}, \qquad \sum_{\alpha=1}^{8} \boldsymbol{\xi}_\alpha \otimes \boldsymbol{T}\,\boldsymbol{\xi}_\alpha = \boldsymbol{I},$$

where the 8×8 matrix $\boldsymbol{T}$ has the following block form:

(23) $$\boldsymbol{T} = \begin{pmatrix} \boldsymbol{0} & \boldsymbol{I} \\ \boldsymbol{I} & \boldsymbol{0} \end{pmatrix}.$$

In order to give formulas for the boundary conditions and the solution itself, we have to define the following partition of the eigenvectors $\boldsymbol{\xi}_\alpha$, the generalized line defect strength $\boldsymbol{g}$, and the solution $\boldsymbol{\eta}$:

(24) $$\boldsymbol{\xi}_\alpha = \begin{pmatrix} \boldsymbol{U}_\alpha \\ \boldsymbol{V}_\alpha \end{pmatrix} = \begin{pmatrix} \boldsymbol{A}_\alpha \\ \varphi_\alpha \\ \boldsymbol{L}_\alpha \\ D_\alpha \end{pmatrix}, \quad \boldsymbol{g} = \begin{pmatrix} \boldsymbol{b} \\ \Delta\varphi \\ -\boldsymbol{f} \\ q \end{pmatrix},$$

(25) $$\boldsymbol{\eta}(k,y) = \begin{pmatrix} \boldsymbol{U}(k,y) \\ \boldsymbol{V}(k,y) \end{pmatrix} = \begin{pmatrix} \boldsymbol{u}(k,y) \\ \varphi(k,y) \\ \boldsymbol{J}(k,y) \\ D(k,y) \end{pmatrix}.$$

There is no risk of confusing $\boldsymbol{U}_\alpha$ with $\boldsymbol{U}(k,y)$ and $\boldsymbol{V}_\alpha$ with $\boldsymbol{V}(k,y)$, because components of the solution $\boldsymbol{\eta}$ are always accompanied by respective variables and have no subscript indices. Given the above notation we can define the so-called boundary representation of the solution $\boldsymbol{\eta}$ and of the eigenvectors $\boldsymbol{\xi}_\alpha$

(26) $$\boldsymbol{\xi}^{(j)\pm}_\alpha = \begin{pmatrix} \boldsymbol{U}^{(j)\pm}_\alpha \\ \boldsymbol{V}^{(j)\pm}_\alpha \end{pmatrix} = \begin{pmatrix} \boldsymbol{A}_\alpha \\ \varphi_\alpha \pm D_\alpha \big/ i\varepsilon^{(j)} \\ \boldsymbol{L}_\alpha \\ D_\alpha \pm i\varepsilon^{(j)}\varphi_\alpha \end{pmatrix},$$

(27) $$\boldsymbol{\eta}^{\pm}(k,y^{(j)}) = \begin{pmatrix} \boldsymbol{U}^{\pm}(k,y^{(j)}) \\ \boldsymbol{V}^{\pm}(k,y^{(j)}) \end{pmatrix} = \begin{pmatrix} \boldsymbol{u}(k,y^{(j)}) \\ \varphi(k,y^{(j)}) \pm D(k,y^{(j)}) \big/ i\varepsilon^{(j)} \\ \boldsymbol{J}(k,y^{(j)}) \\ D(k,y^{(j)}) \pm i\varepsilon^{(j)}\varphi(k,y^{(j)}) \end{pmatrix},$$

where $\pm = (-1)^{j+1} sgn(k)$. The boundary representation allows us to express the mixed boundary conditions in a very simple form [2]

(28) $$\boldsymbol{U}^{\pm}(k,y^{(1)}) = 0, \quad \boldsymbol{V}^{\pm}(k,y^{(2)}) = 0,$$

where the first relation means that at $y=y^{(1)}$ the boundary is clamped, and the second relation means that at $y=y^{(2)}$ the boundary is mechanically free. Moreover, these conditions guarantee continuity of the normal component of the electric displacement field. It can be shown that given Eqs. (28) the final solution has the form

(29) $$\begin{pmatrix} \boldsymbol{\beta} \\ \mathbf{E} \end{pmatrix} = \int_{-\infty}^{\infty} \frac{dk}{2\pi} \sum_{\alpha,\beta=1}^{8} e^{ik\left[x - x' + p_\alpha\left(y - y^{(1)}\right) - p_\beta\left(y' - y^{(1)}\right)\right]} \times$$
$$\times (\boldsymbol{m} + p_\alpha \boldsymbol{n}) \otimes \begin{pmatrix} \boldsymbol{A}_\alpha \\ -\varphi_\alpha \end{pmatrix} \left[m_{\alpha\beta} - \delta_{\alpha\beta} H(y - y')\right] \boldsymbol{\xi}_\beta \cdot \boldsymbol{g},$$

(30) $$m_{\alpha\beta}(k) = \begin{cases} m^{(+)}_{\alpha\beta}(k), & k < 0, \\ m^{(-)}_{\alpha\beta}(k), & k > 0, \end{cases}$$

(31) $$m^{\pm}_{\alpha\beta}(k) = \boldsymbol{V}^{(1)\pm}_\alpha \cdot \left(\sum_{\gamma=1}^{8} \boldsymbol{V}^{(2)\pm}_\gamma \otimes \boldsymbol{V}^{(1)\pm}_\gamma e^{ikd\left(p_\gamma - p_\beta\right)} \right)^{-1} \boldsymbol{V}^{(2)\pm}_\beta .$$

This rather complicated set of equations allows numerical evaluation of the elastic distortion field $\boldsymbol{\beta}$ and the electric field $\boldsymbol{E}$. The stress field $\boldsymbol{\sigma}$ and the electric displacement field can be computed more easily, using the constitutive relations given by Eq. (13).

Results of numerical experiments

For our experiments GaAs as the material of the layer was chosen. Symmetry class of GaAs is cubic, and the corresponding material constants are as follows: c_{11}=119 GPa, c_{12}=53.4 GPa, c_{44}=5.96 GPa, e_{14}=-0.16 C/m^2, ε_{11}=12.9 ε_0, where ε_0 is the dielectric permittivity of the vacuum. It was assumed that the layer thickness d equals 0.5 μm, and that relative dielectric permittivities are ε_1=1.13 ε_0 and ε_1=2.26 ε_0. The first constant may be the one of a slightly contaminated gas, while the second one corresponds to a polymer (e.g. polypropylene or polyethylene) background structure. In the applied coordinate system the upper boundary at -0.25 μm is clamped, and the lower boundary at 0.25 μm is mechanically free. For such a setup we have computed the physical fields $\boldsymbol{E}$, $\boldsymbol{D}$, $\boldsymbol{\beta}$, $\boldsymbol{\sigma}$ for 30 equidistant locations of the defect, spanning from one boundary to the other. Results for all possible types of defect sources (dislocation, line force, line charge, potential jump) were computed. As hundreds possible pairs (defect source, resultant physical field component) are possible, in Figs. 2-5 below only some selected, typical results are presented: the fields $\boldsymbol{\beta}$, $\boldsymbol{\sigma}$ are induced by a dislocation with $\boldsymbol{b}$ = (0, 1 nm, 0), and the fields $\boldsymbol{E}$, $\boldsymbol{D}$ are induced by a line force with $\boldsymbol{f}$ = (0, 10^{-5} $N/\mu m$, 0). Hence, we

show the cross-effect being the essence of piezoelectricity. The Burgers vector is of magnitude of $1\ nm$ which corresponds to a slip of approximately twice the GaAs lattice constant, and assumed magnitude of the line force is moderate for this system.

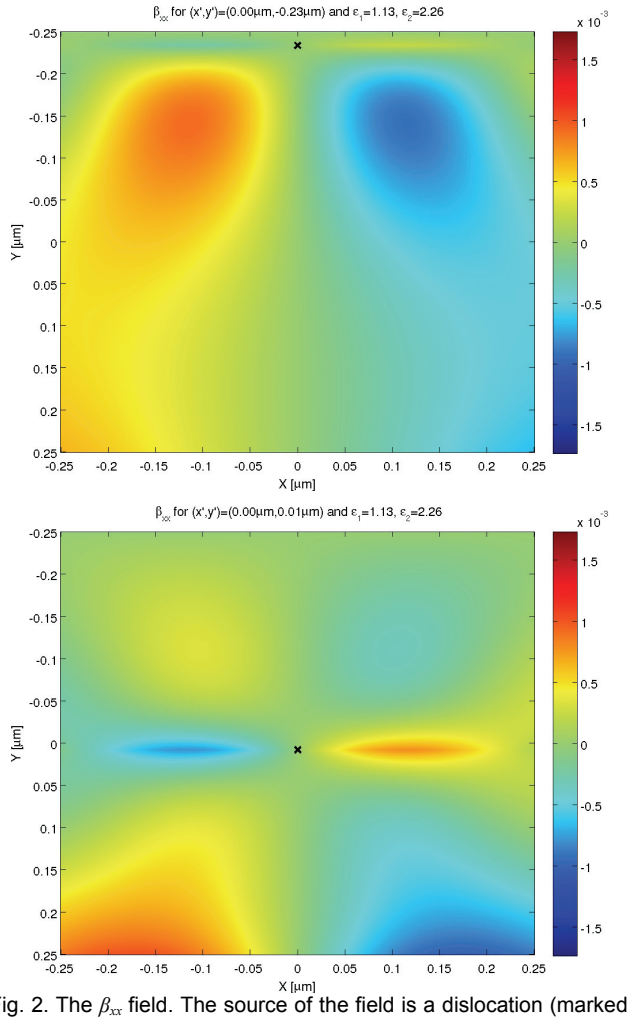

Fig. 2. The β_{xx} field. The source of the field is a dislocation (marked with $\times$) with Burgers vector $\boldsymbol{b} = (0,\ 1\ nm,\ 0)$.

It is seen that at y=-0.25 μm there are no displacements, as expected. On the contrary, at y=-0.25 μm displacements are of considerable value.

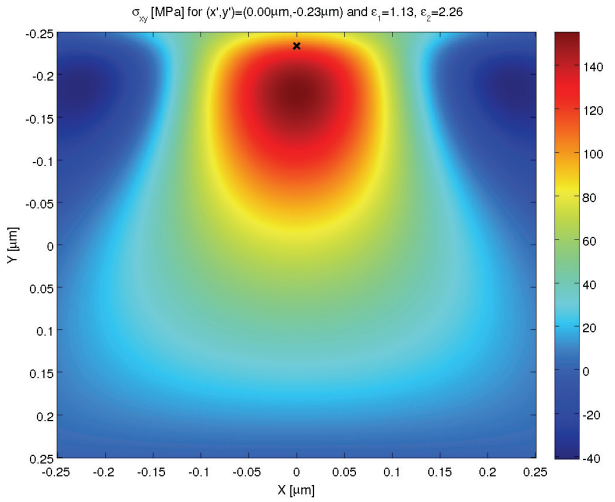

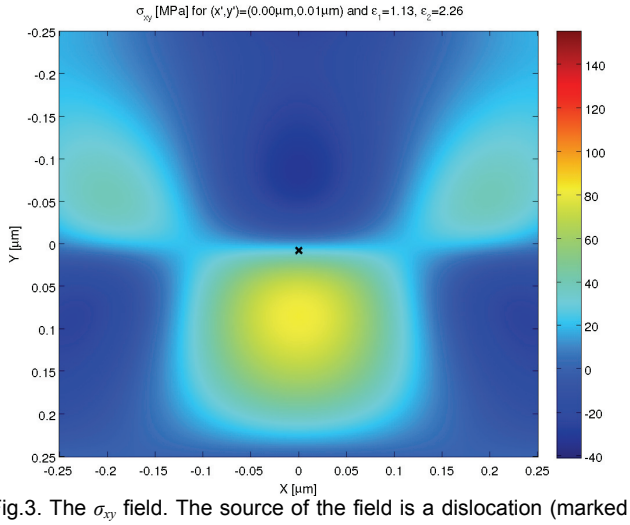

Fig.3. The σ_{xy} field. The source of the field is a dislocation (marked with $\times$) with Burgers vector $\boldsymbol{b} = (0,\ 1\ nm,\ 0)$.

The situation is exatcly opposite in the case of stresses. It is seen that at y=-0.25 μm stresses are substantial and therefore cannot be disregarded in practical applications, and at y=0.25 μm no stress is observed since this boundary is assumed to be mechanically free.

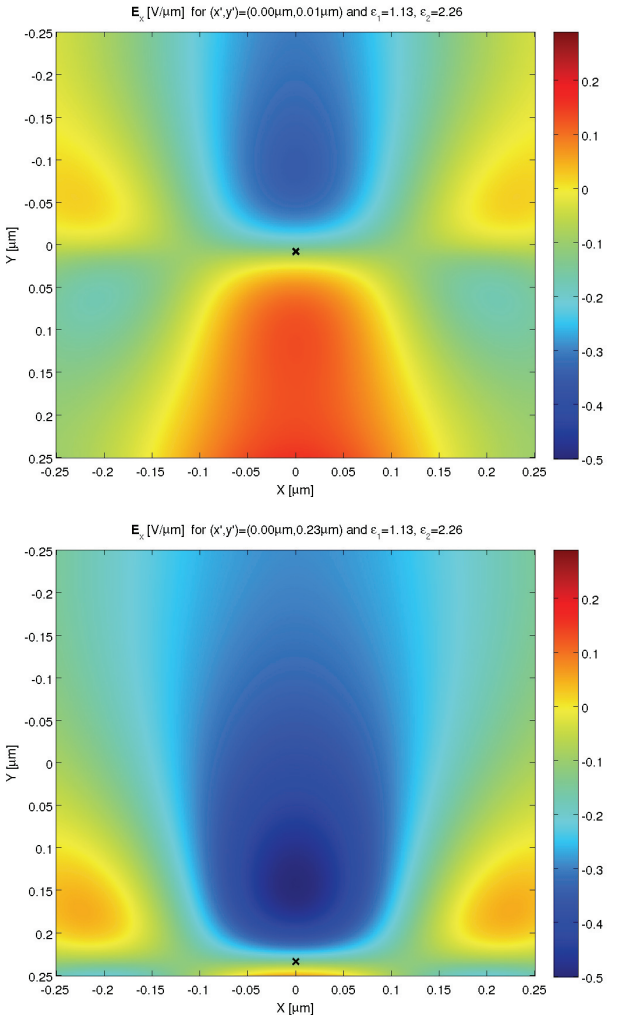

Fig. 4. The E_x field. The source of the field is a dislocation (marked with $\times$) with line force vector $\boldsymbol{f} = (0,\ 10^{-5}\ N/\mu m,\ 0)$.

In general, the electric field does not vanish in either point of the structure. This field is essential when the internal structure of the material is considered. High values or high gradients of this field may translate into reduced durability and stability of structures which are engineered for manufacturing. Therefore the content of the above plots should be taken into consideration during sustainability analysis.

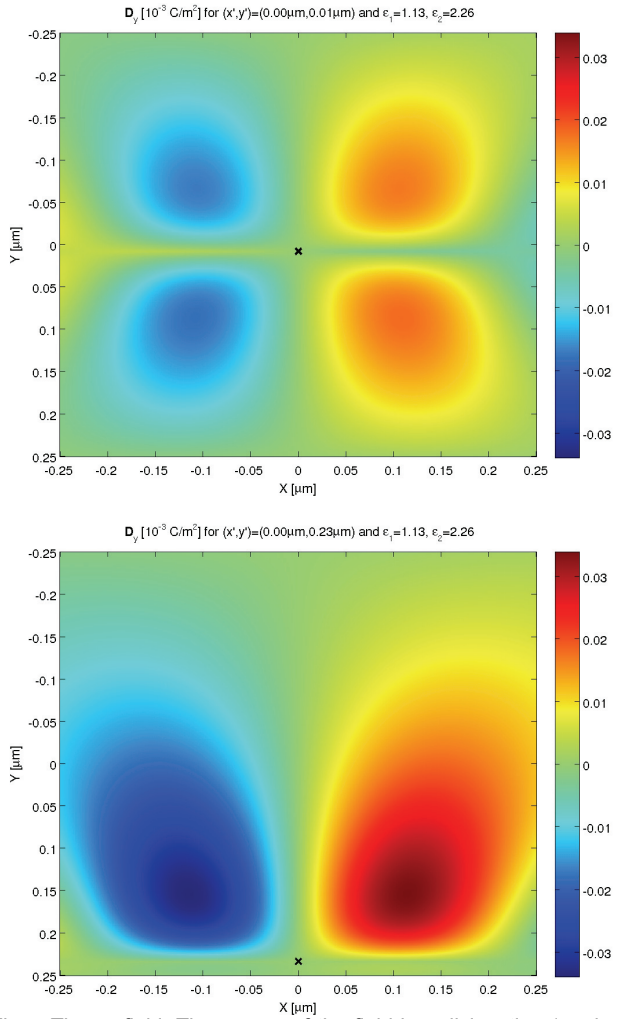

Fig.5. The D_y field. The source of the field is a dislocation (marked with $\times$) with line force vector $\boldsymbol{f} = (0, 10^{-5}\ N/\mu m, 0)$.

The electric displacement field vanishes at both boundaries, and this fact is a clear consequence of boundary conditions (28) where continuity of the dielectric displacement component normal to the boundary of the plate is implicitly assumed. It is well known that the dielectric displacement field governs behavior of free electric charges which carry information collected by the device. Therefore values of this field directly influence the response pattern of the plate as an active element in an electronic device.

Conclusions

2D color-coded plots depicting electro-elastostatic fields of a single defect in a thin layer of GaAs were presented. One boundary of the layer was clamped to the substrate and the other was mechanically free. The observed plots allow to conclude about usual magnitudes of the piezoelectric cross-effect for typical parameters of the defect. Obtained values show that the parasitic fields induced by defects in thin layers must be taken into consideration when designing electronic devices in which such structures are to be implemented.

Acknowledgments

This paper was supported by the grant number N501 252334 of the Polish Foundation of Science and Higher Education (MNiSW).

REFERENCES

[1] Nowacki J.P., Alshits V.I., Radowicz A., 2D electro-elastic fields in a piezoelectric layer–substrate structure, *Int. J. Eng. Sci.*, 40 (2002), 2057-2076

[2] Nowacki J.P., Static and dynamic coupled fields in bodies with piezoeffects or polarization gradient, *LNCS 26*, 2006

[3] Eibl O., Peranio N., Stress, strain and electric field calculation for dislocations and their contrast under two-beam conditions: implementation in Matlab, *Microscopy and Microanal.*, 13 (2007), 352-353

[4] Stroh S.N., Steady state problems in anisotropic elasticity, *J. Math. Phys.*, 41 (1962), 77-103

[5] Barnett D.M., Lothe J., Dislocations and line charges in anisotropic piezoelectric insulators, *Phys. Stat. Sol. (b)*, 67 (1975), 105-111

***Authors**: mgr Konrad Bojar, Industrial Research Institute for Automation and Measurements, Laboratory of Autonomous Defense Systems, al. Jerozolimskie 202, 02-486 Warsaw, Poland, e-mail: kbojar@piap.pl,*

prof. dr hab. Vladimir Alshits, Institute of Crystallography RAS, Moscow, Leninskii prospekt 59, Moscow, 119333 Russia, e-mail: alshits@ns.crys.ras.ru,

dr Jerzy P. Nowacki, Polish-Japanese Institute of Information Technology, Koszykowa 86, 02-008 Warsaw, Poland, e-mail: jnowacki@pjwstk.edu.pl,

dr Aldona Drabik, Polish-Japanese Institute of Information Technology, Koszykowa 86, 02-008 Warsaw, Poland, e-mail: adrabik@pjwstk.edu.pl,

prof. dr hab. Romuald Kotowski, The State College of Computer Science and Business Administration, Akademicka 14, 18-400 Łomża, Poland, e-mail: rkotowski@pwsip.edu.pl